

# Comparative between Behaviour of Single Floating Reinforced Stone Column and Single Pile under Axial Load

Haifaa A. Ali<sup>1</sup>, Mohammed S. Jabbar<sup>2</sup>

<sup>1</sup>Assist Professor, Instructor, College of Engineering, University of Baghdad Iraq

<sup>2</sup>Researcher, College of Engineering, University of Baghdad Iraq

**Abstract:** In this work, three-dimensional finite, element, analysis of single, floating reinforced, stone, column, (FRSC) and, pile foundation under axial load analyzed using PLAXIS (3D) 2013. The hardening soil and Mohr-Coulomb models are used to simulate the behaviour of clayey soil and FRSC respectively. While linear elastic model is used to simulate the behaviour of structures (pile, footing and geo-grid). Two types of pile foundation are studied, bored and driven concrete pile, the parametric study including the changing of length and diameter of (FRSC) and bored pile; however, the driven pile has constant cross section (28 x 28) mm. For FRSC and bored pile two lengths (6 and 12) m and three diameters (0.4, 0.6 and 0.8) m are analyzed. From the results of finite element analysis, the bored pile has clear advantage of improvement over the driven pile and FRSC, the results of the improvement using the FRSC were better than the driven pile.

**Keywords:** Finite element, floating reinforced stone column, axial load, bored pile, driven pile, improvement

## 1. Introduction

Ground improvement is the modification of foundation soils or project earth structures to provide better performance under operational loading conditions [1]. Soft soil deposits are extensively found in many marginal regions and they have low strength and high compressibility. Stone column that consist of granular material compacted in long cylindrical holes is used as a technique for enhancing the strength and consolidation characteristics of soft clays [2]. The load carrying capacity of the stone column depends on the lateral confining pressure from the surrounding soils. In very soft clays, ordinary stone columns do not achieve significant load carrying capacity due to low lateral confinement. Therefore, stone columns of additional confinement are needed for the better performance [3-5]. In recent years, geosynthetic reinforced stone columns have been successfully adopted in very soft soils throughout the world. Vertical encased stone columns have several advantages like increased stiffness of column by mobilization of hoop stress in the reinforced material, preventing the loss of stones into the surrounding soft clay, preserving the drainage and frictional properties of the stone aggregates. Numerical analyses have performed by various researchers on geosynthetic reinforced stone columns, [6-9]. In this study, performance of the reinforced stone column was studied with reference to strength and is compared with the performance of piles foundation.

size distribution curve of studied soil and the physical properties of studied soil respectively. All tests were, conducted, at the Postgraduate Laboratory, at the University, of Baghdad.

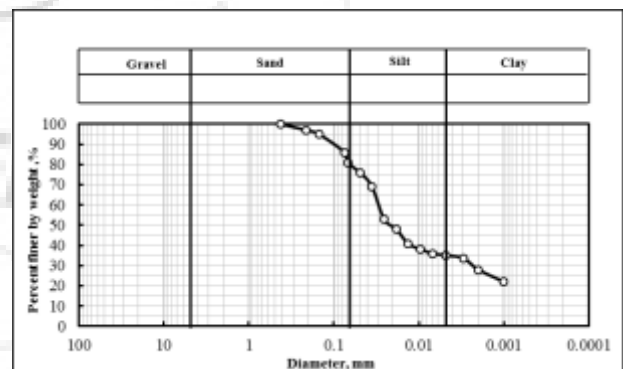


Figure 1 Grain size distribution of the studied soil

Table 1: The physical properties of studied soil.

Soil Parameter	value	Specification
Natural water, content % (wc)	26	ASTM D-2216
Liquid, limit % (LL)	41	ASTM D-4318
Plastic, limit % (PL)	19.5	ASTM D-4318
Plasticity, index % (PI)	21.5	—
Specific, gravity (Gs)	2.69	ASTM D-854
% Fine sand (0.2 to 0.075) mm	14	ASTM
% Silt (0.075 to 0.005) mm	51	ASTM
% Clay (< 0.005 mm)	35	ASTM
Classification of soil	CL	USCS

## 2. The Material Used

### 2.1 The Natural Cohesive Soil

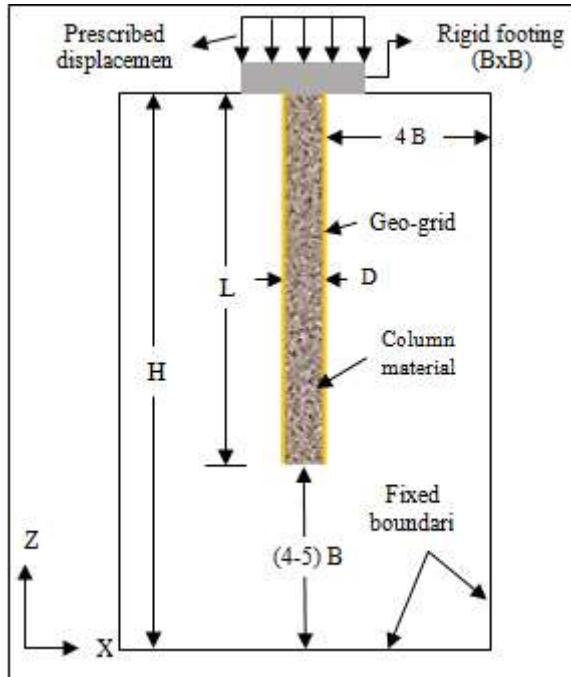
The cohesive soil used in this paper is obtained from Baghdad city from depth (3.5-4) m, below the ground, surface, by Shelby tube sampler as an undisturbed soil sample. Standard laboratory tests were used to obtain its physical properties. Figure 1 and Table 1 are show the Grain

## 3. Model Geometry, Constitutive Models and Input Parameters

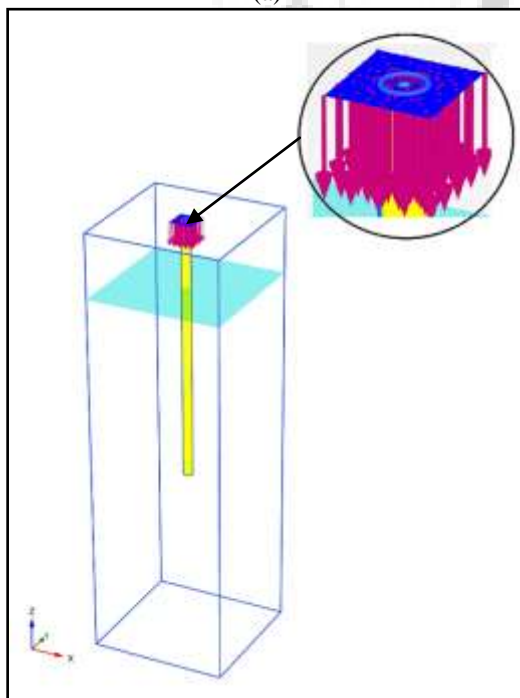
### 3.1 Geometry

The model dimensions were selected to prevent the effect of lateral and lower boundaries on the deformation of system

[10]. Figure 2 illustrate schematic diagram of finite element model. The model consisting of soil domain confining by lateral and lower boundaries, the loading carried by rigid surface square footing (1 x 1) m to cancel the contribution of the embedment depth. Figure 3 shows finite element mesh and nodes of the model. The displacement control approach used to evaluate the load-settlement curve. In this approach the load required to reach the desired displacement can be determined. In this study the prescribed displacement value is (10% B) as recommended in plate loading test (ASTM- D 1194 – 94).



(a)



(b)

**Figure 2 (a and b):** Schematic of the finite element model

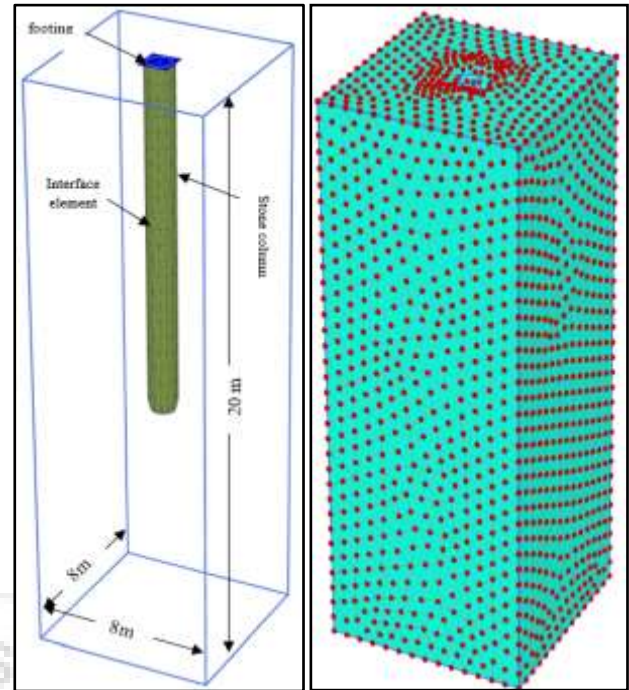


**Figure 3** Finite element mesh and nodes

### 3.2 Constitutive Models, and Input, parameters

PLAXIS 3D provides various constitutive models. In this work, hardening soil model (Brinkgreve 2007) and Mohr-Coulomb model are used for simulation of cohesive soil and stone column respectively, linear elastic model for simulation of structural elements (footing and geo-grid). The parameters of hardening soil model (HSM) are obtained from consolidation drained (CD) triaxial tests (ASTM D7181-11) and oedometer test. Figures 4 and 5 show the Mohr's circles of stress and defining of  $E_{50}^{ref}$  from stress-strain relationship for (100 kPa) reference effective confining stress. Figure 6 shows the definition of  $E_{oed}^{ref}$  from stress-strain relationship of standard oedometer test (ASTM-D2435M – 11). Table 3 shows the parameters of geo-grid reinforcement.

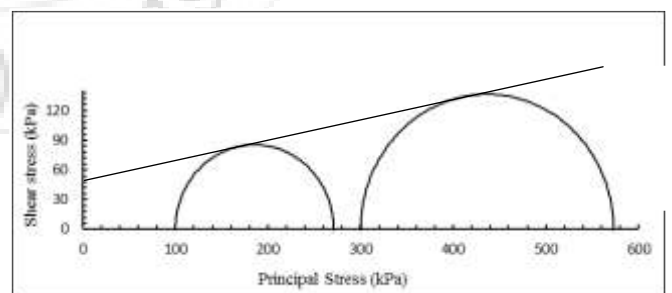


**Figure 4:** Mohr's circles of stress for (100 and 300) effective confining stress

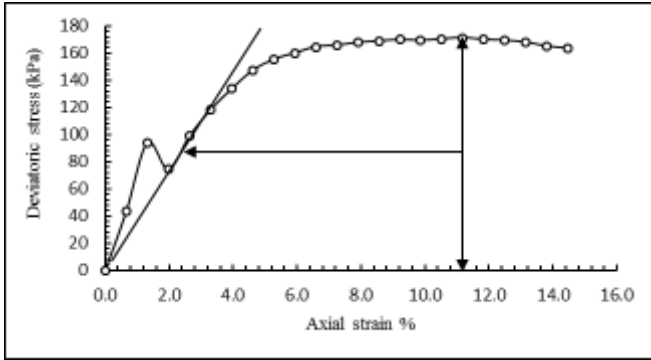


**Figure 5:** Definition of  $E_{50}^{ref}$  from Stress-strain relationship of triaxial (CD) test for (100) kPa effective confining stress

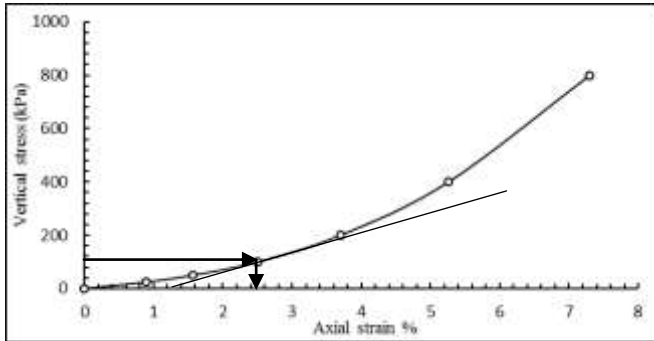


**Figure 6:** Definition of  $E_{oed}^{ref}$  from stress-strain of the standard oedometer test

**Table 2:** Input parameters for the studied soil and stone

Properties	Cohesive soil	Stone [11]
Unsaturated unit weight, $\gamma_{unsat}$ ( $kN/m^3$ )	16	14.4
Saturated unit weight, $\gamma_{sat}$ ( $kN/m^3$ )	18.5	15.7
Material model	Hardening soil	Mohr-Coulomb
Drainage type	Undrained(A)	drained
E (kPa)	—	150000
$E_{50}^{ref}$ (kPa)	3886	—
$E_{oed}^{ref}$ (kPa)	6600	—
$E_{ur}^{ref}$ (kPa)	11658	—
Cohesion, $c'$ (kPa)	48	1
Friction angle, $\phi'$ (degree)	12	41.5
Interface stiffness ratio, $R_{int}$	0.98	0.96

**Table 3** Parameters of geo-grid reinforcement [12]

Geo-grid	Axial Stiffness EA (kN/m)	Aperture size (mm x mm)
G	240	40x28

## 4. Result and Discussion

### 4.1 Analysis of square footing resting on the untreated soil

The bearing capacity of studied soil is evaluated numerically using PLAXIS 3D 2013. Load- settlement relationships a direct method for obtaining ultimate bearing capacity [13]. Figure 7 shows the load-settlement relationship of single isolated footing resting on the untreated soil. Table 4 shows the value of ultimate bearing capacity of the untreated soil

from load-settlement curve defined according to (0.1B) method.

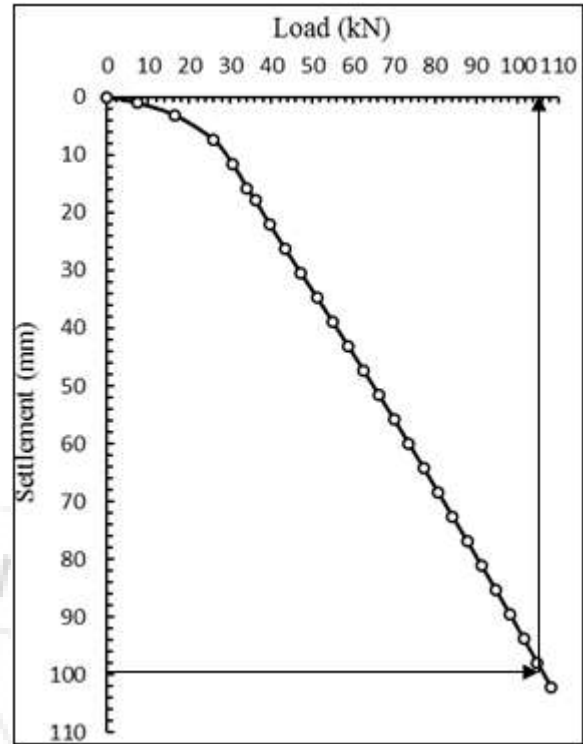


**Figure 7:** The load-settlement relationship of single isolated footing resting on the untreated soil.

**Table 4** ultimate bearing capacity of the untreated soil

Ultimate capacity	Value (kPa)
The untreated soil	106

### 4.2 Comparative between results of single FRSC and pile foundation

The load-settlement curves of single FRSC, single bored and driven pile are compared with the untreated soil. The comparison is conducted between the elements have the same length and diameter; however, driven pile is compared with element has the same length only.

The ratio of column's to footing's area is defined as area replacement ratio (AR).

$$Ar = \frac{A_c}{A_f}$$

Where:

$A_c$ : area of stone column or bored pile  
 $A_f$ : area of footing (one square meter)

The increasing of bearing capacity as a result of stone column installation has been included in bearing capacity ratio (BCR), [14].

$$BCR = \frac{q}{q_o}$$

Where

$q$ : ultimate bearing capacity of treated soil  
 $q_o$ : ultimate bearing capacity of untreated soil

The final deformed shape of finite element model is illustrated in figure 8 (a and b), figure (8a) shows the

deformation of FRSC a combined failure (penetrating and bulging) [15] occurs under footing load, while, only penetrating failure occurs in bored pile because of the high rigidity of concrete material.

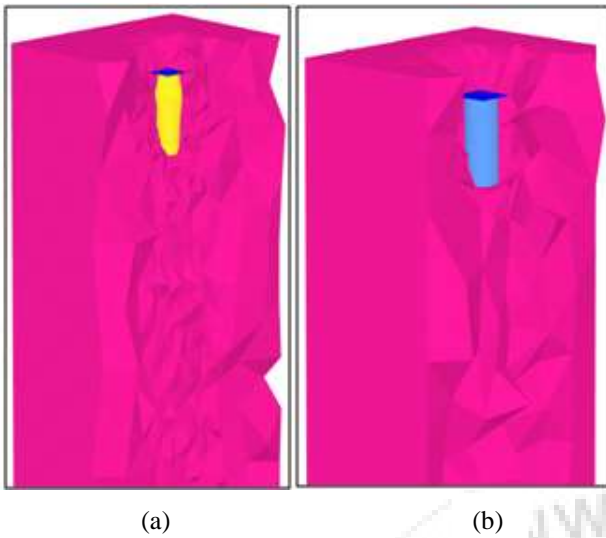


**Figure 8 (a, b):** Vertical cross section through the deformed shape of the FRSC and the bored pile respectively

Figures (9) to (14) are show the load-settlement relationships of single FRSC and pile foundation for (6 and 12) m length

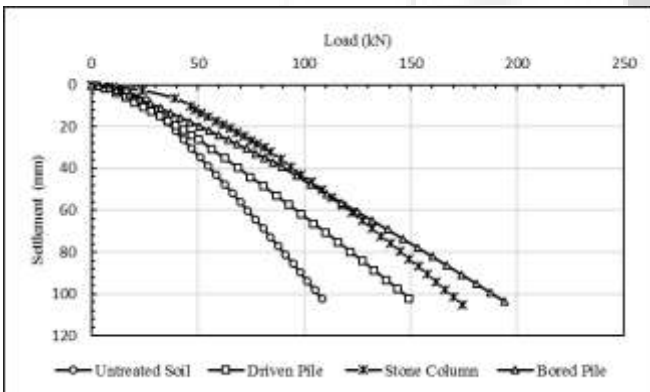


**Figure 9:** Load-settlement relationships of single FRSC and pile foundation for (L= 6) m and (L/D) =15

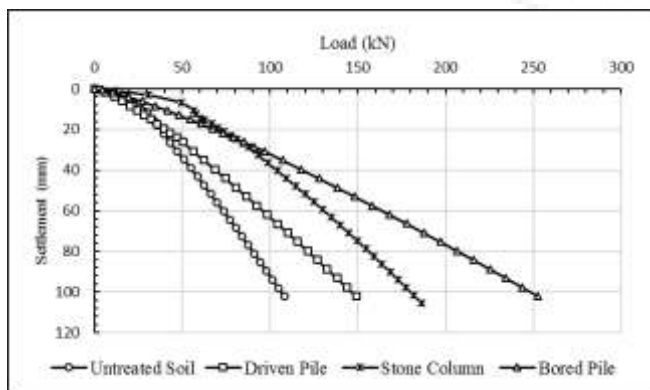


**Figure 10:** Load-settlement relationships of single FRSC and pile foundation for (L= 6) m and (L/D) =10

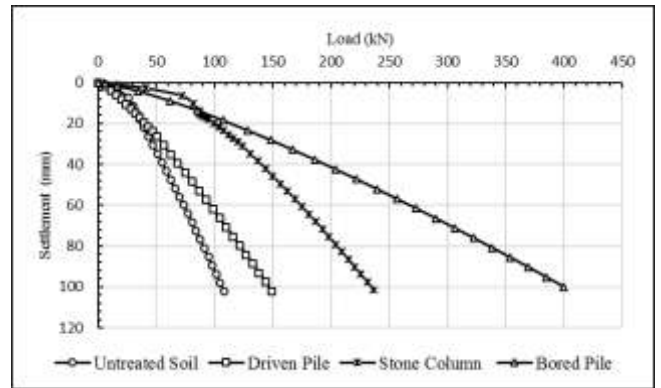


**Figure 11:** Load-settlement relationships of single FRSC and pile foundation for (L= 6) m and (L/D) =5.7

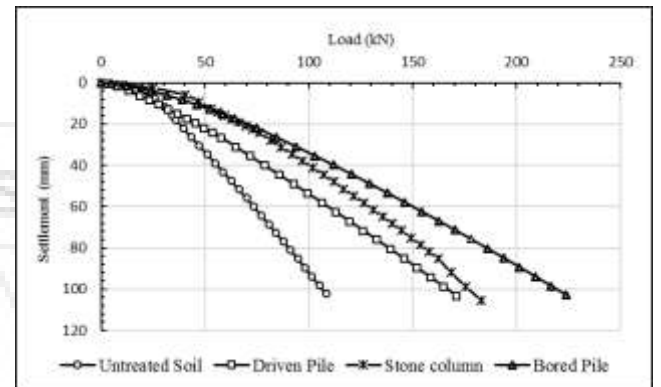


**Figure 12:** Load-settlement relationships of single FRSC and pile foundation for (L=12) m and (L/D) =30

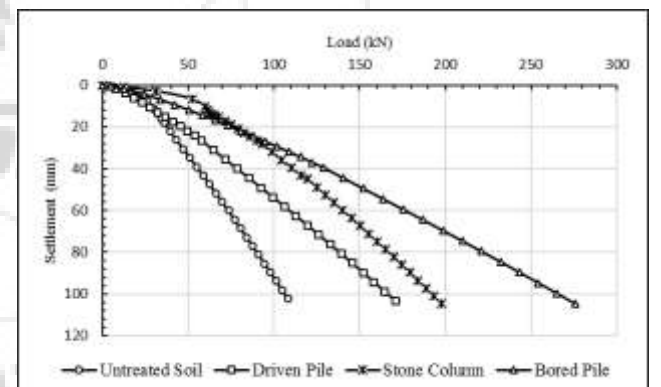


**Figure 13:** Load settlement relationships of single FRSC and pile foundation for (L=12) m and (L/D) =20

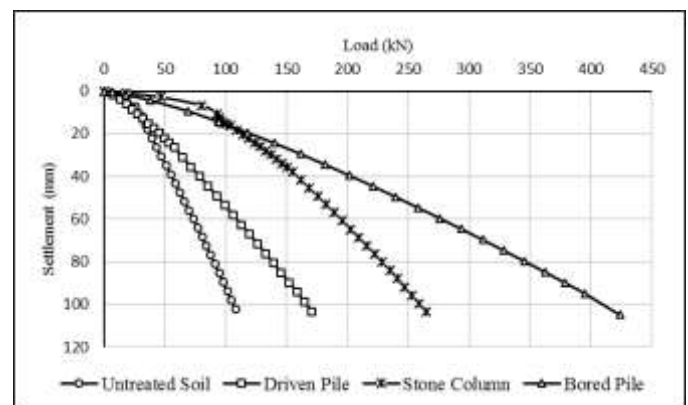


**Figure 14:** Load settlement relationships of single FRSC and pile foundation for (L=12) m and (L/D) =15

Figures 15 and 16 show the relationship between BCR and AR for FRSC (6 and 12) m length respectively. Figures (9) to (14) clearly show that the capacity of single FRSC is increases with the increasing of column length, and for the same length columns the capacity increase with the increasing of column's diameter. bored pile has a clear advantage of improvement over the driven pile and FRSC, the results of the improvement using the FRSC were better than the driven pile. Figures 15 and 16 are show that the area ratio has clear effect on the BCR of FRSC

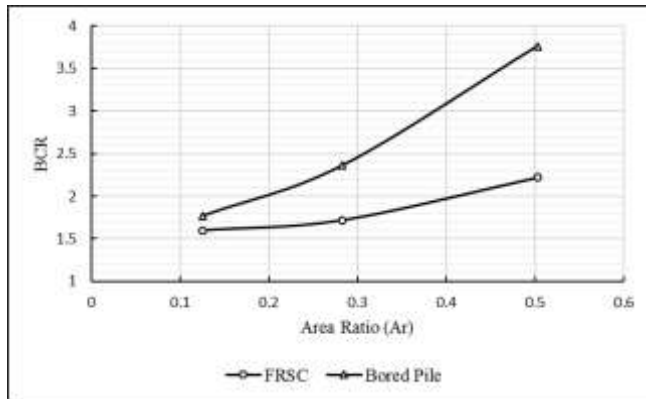


**Figure 15** Influence of area ratio on BCR of single FRSC for (6) m length

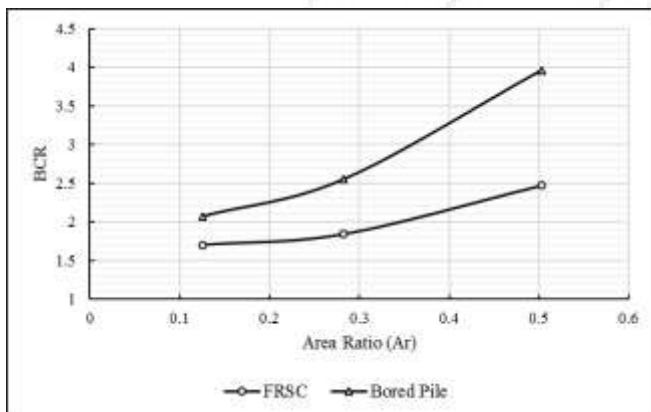


**Figure 16:** Influence of area ratio on BCR of single FRSC for (12) m length

## 5. Conclusions

According to the finite element analysis of floating reinforced stone column and piles foundation as mentioned previously. The following points are concluded:

- 1) In small diameters bored piles (D less than 0.5 m), the ultimate load is a bout (1.1-1.2) times the ultimate load capacity of floating reinforced stone column.
- 2) The ultimate load capacity of floating reinforced stone column (D=0.6) m is about (1.14-1.22) times the ultimate capacity of driven pile.
- 3) For the large diameters bored piles (D larger than 0.5 m), The ultimate load capacity is a bout (1.6-1.7) times the ultimate load capacity of floating reinforced stone column.
- 4) The floating reinforced stone columns are failed in combined failure (bulging and penetrating), while the bored piles failed only with penetrating failure.

## References

- [1] Gáb, M., Schweiger, H. F., Kamrat-Pietraszewska, D., &Karstunen, M. (2008, August). Numerical analysis of a floating stone column foundation using different constitutive models. In *Proceedings of the 2nd International Workshop on the Geotechnics of Soft Soils-Focus on Ground Improvement* (pp. 137-142).
- [2] Malarvizhi, S.N. and Ilamparuthi, K. (2004), Load Versus Settlement of Clay-Bed Stabilized with Stone and Reinforced Stone Columns, Proceedings of the 3rd Asian Regional Conference on Geosynthetics, GEOASIA, Seoul, Korea, pp. 322-329.
- [3] M. Hasan and N. K. Samadhiya, 2017. Performance of geosynthetic-reinforced granular piles in soft clays: Model tests and numerical analysis. *Computers and Geotechnics*, 87, 178-187.
- [4] Barksdale RD, Bachus RC. Design and construction of stone columns. Federal highway administration RD, 83/026; 1983.
- [5] Mitchell JK, Huber TR. Performance of a stone column foundation. *J GeotechEng ASCE* 1985;111(2):205-23.
- [6] 6- MicheálM.Killeena and Bryan A. McCabe, 2014. Settlement performance of pad footings on soft clay supported by stone columns: A numerical study. 0038-0806/& 2014 The Japanese Geotechnical Society.
- [7] Killeen, M.M., 2012.Numerical modelling of small groups of stone columns (Ph.D. thesis). National University of Ireland, Galway.
- [8] Mitchell, J.K., Huber, T.R., 1985.Performance of a stone column foundation. *J. Geotech. Eng., ASCE*11(2),205-223.
- [9] J. Gniel and A. Bouazza, 2009. Numerical modelling of small-scale geogrid encased sand column tests. *Geotechnics of Soft Soils*, 2009 Taylor & Francis Group, London.
- [10] Narasimha Rao, S., Madhiyan, M. and Prasad, Y. V. S. N. (1992). Influence of bearing area on the behaviour of stone columns. *Indian Geotechnical Conf.*, Calcutta, 235-237.
- [11] Al-Shammari H. A. (2013) "An Experimental and Theoretical Study on Ordinary and Encased Stone Columns Underneath Embankment", Ph.D. Thesis, Civil Engineering Department, University of Baghdad, Iraq.
- [12] Fattah, M. Y., Al-Omari, R. R., & Ali, H. A. (2015). Numerical Simulation Of The Treatment Of Soil Swelling Using Grid Geocell Columns. *Slovak Journal of Civil Engineering*, 23(2), 9-18.
- [13] A. J. Lutenegeger and M. T. Adams, "Bearing capacity of footings on compacted sand," in *Proceedings of the 4th International Conference on Case Histories in Geotechnical Engineering*, pp. 1216-1224, 1998.
- [14] Bhattacharjee, A., Mittal, S., & Krishna, A. (2011). Bearing capacity improvement of square footing by micropiles. *International Journal of Geotechnical Engineering*, 5(1), 113-118.
- [15] Greenwood D.A. (1970), "Mechanical Improvement of Soils Below Ground Surface.", Conf., Institute of Civil Engineers, June, pp.11-22.